

Thermal Conductivity of Mg-doped CuGeO₃

J. Takeya, I. Tsukada and Yoichi Ando

Central Research Institute of Electric Power Industry, Komae, Tokyo 201-8511, Japan

T. Masuda and K. Uchinokura

Department of Advanced Materials Science, The University of Tokyo, 7-3-1, Hongo, Bunkyo-ku, Tokyo 113-8656, Japan

(Received)

The thermal conductivity κ is measured in a series of Cu_{1-x}Mg_xGeO₃ single crystals in magnetic fields up to 16 T. It has turned out that heat transport by spin excitations is coherent for lightly doped samples, in which the spin-Peierls (SP) transition exists, at temperatures well above the SP transition temperature T_{SP} . Depression of this spin heat transport appears below T^* , at which the spin gap *locally* opens. T^* is not modified with Mg-doping and that T^* for each Mg-doped sample remains as high as T_{SP} of pure CuGeO₃, in contrast to T_{SP} which is strongly suppressed with Mg-doping. The spin-gap opening enhances phonon part of the heat transport because of reduced scattering by the spin excitations, producing an unusual peak. This peak diminishes when the spin gap is suppressed both in magnetic fields and with the Mg-doping.

PACS numbers: 66.70.+f, 75.30.Kz, 75.50.Ee

I. INTRODUCTION

The discovery of the first inorganic spin-Peierls (SP) compound CuGeO₃ (Ref. 1) has triggered subsequent studies of the impurity-substitution effect on the spin-singlet states,² and the existence of the disorder-induced transition into three-dimensional antiferromagnetic (3D-AF) state has been established.^{3,4} Since the relevant exchange energies, i.e., intra- and interchain coupling J and J' , do not change with doping except at the impurity sites, it is difficult to understand the impurity-induced transition from the SP to 3D-AF state in the framework of the “conventional” competition between dimensionalities (where J'/J is an essential parameter⁵) and therefore such impurity-substitution effect is a matter of current interest.

In CuGeO₃, a small amount of impurity leads to an exotic low-temperature phase where the lattice dimerization and antiferromagnetic staggered moments simultaneously appear [dimerized AF (D-AF) phase].⁶ Moreover, when the impurity concentration x exceeds a critical concentration x_c , the SP transition measured by dc susceptibility disappears^{7,8} and a uniform AF (U-AF) phase appears below the Néel temperature $T_N \sim 4$ K.⁶ The D-AF ground state can be understood as a state of spatially modulated staggered moments accompanied with the lattice distortion.^{9,10} However, the mechanism of the depression of the SP phase and the establishment of the disorder-induced antiferromagnetism are still to be elucidated. A transport measurement could be a desirable tool in dealing with such a problem, because the mobility of spin excitations or spin diffusivity is often sensitive to the impurities. Nevertheless, even a crude estimation of the mobility has not been carried out for the spin excitations so far.

Recently, we reported intriguing behaviors of the thermal conductivity κ of pure CuGeO₃.¹¹ In Ref. 11, the

existence of the spin heat channel (κ_s) was suggested. However, we cannot separate κ_s and the phonon thermal conductivity κ_{ph} with the measurement of the pure sample only. In this work, we have resolved this problem with Mg-doped crystals. It turned out that the spin diffusion length, which can be calculated from κ_s , is much larger than the distance between adjacent spins for the pure CuGeO₃, indicating coherent heat transport due to the spin excitations. Since the spin heat transport almost disappears for the heavily doped samples in which the long-range SP ordering is absent, it is suggested that the large mobility of the spin excitations plays an important role in the SP ordering.

The spin heat transport is also a probe of the spin gap. It is found that local spin-gap opening is robust against the impurity doping, though the temperature of the long-range ordering is strongly suppressed with x . Phonon heat channel (κ_{ph}) provides an unusual thermal conductivity peak in the SP state, which was one of the topics of our previous report.¹¹ The peak is drastically suppressed with both magnetic field and Mg-doping, indicating that the spin-gap opening has produced the peak in κ_{ph} via strong phonon-spin interaction.

II. EXPERIMENTAL

The single crystals of Cu_{1-x}Mg_xGeO₃ were grown with a floating-zone method. The Mg concentration is determined by inductively coupled plasma-atomic emission spectroscopy (ICP-AES).⁶ The critical concentration x_c was carefully determined by Masuda *et al.* for the same series of crystals that we have used.^{6,12} They found that the Néel temperature T_N jumps at the impurity-driven transition from D-AF to U-AF phase and that phase is separated in the transition range of $0.023 \leq x \leq 0.027$, indicating that the transition is of first order.^{6,12} We used

six samples with $x = 0$, $0 < x < x_c$, and $x > x_c$ for the thermal conductivity measurement. They were originally prepared for the neutron and the synchrotron x-ray experiments, and thus the sample homogeneity has been confirmed in detail which is described elsewhere.¹² Typical sample size is $0.2 \times 2 \times 7 \text{ mm}^3$ ($a \times b \times c$). Since our interest is thermal conductivity along the 1D spin chain, we need the sample with a longer dimension along the c axis. Thus we paid particular attention to the Mg homogeneity along the c axis for this study, and the best way is to use the samples prepared for the neutron experiments. The fundamental magnetic properties of the samples used already appeared in another paper.¹²

The thermal conductivity is measured using a “one heater, two thermometers” method as the previous measurement.¹¹ The base of the sample is anchored to a copper block held at desired temperatures. A strain-gauge heater is used to heat the sample. A matched pair of microchip Cernox thermometers are carefully calibrated and then mounted on the sample. The maximum temperature difference between the sample and the block is 0.2 K. Typical temperature difference between the two thermometers is ~ 0.5 K above 20 K and 0.2 K below 20 K. The temperature-controlled block is covered with a metal shield so that heat loss through radiation becomes negligible. Magnetic field is applied parallel to the c -axis direction. The measured temperature range is below 30 K, which is well below the temperature scale of the intra-chain coupling J_c (~ 120 K according to neutron scattering measurement¹³), and therefore, the one-dimensional quantum spin liquid (1D-QSL) is realized above the transition temperatures.

III. RESULTS

Figure 1 shows the temperature dependence of κ for samples with and without Mg substitution: 1(a)-1(f) are for $x = 0$, 0.016, 0.0216, 0.0244, 0.032 and 0.040, respectively. $x = 0.016$ is well below x_c , $x = 0.0216$ is close to x_c , $x = 0.0244$ is on the border and $x = 0.032$ and $x = 0.040$ are in the U-AF region. The transition temperatures T_{SP}^x for the $x \leq x_c$ samples and T_N for the $x > x_c$ samples, which were determined by susceptibility measurement,¹² are indicated by arrows in the figures. A sharp drop is observed just below T_{SP}^x for the pure CuGeO_3 as presented in the inset of Fig. 1(a). The $x = 0.016$ sample shows the same behavior at T_{SP} , while κ is *enhanced* just below T_{SP} for the $x = 0.0216$ and 0.0244 samples.

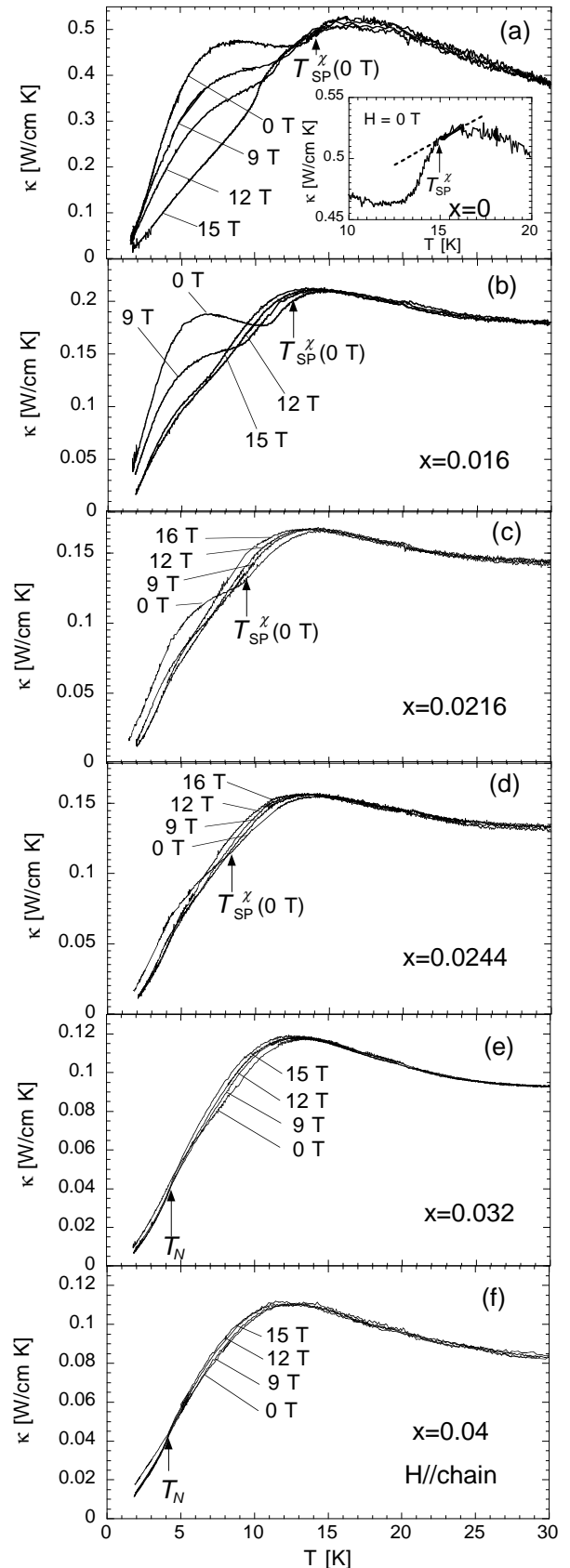


FIG. 1. Thermal conductivity of $\text{Cu}_{1-x}\text{Mg}_x\text{GeO}_3$ single crystals in magnetic fields up to 15 or 16 T applied along the chain direction, for (a) $x = 0$, (b) $x = 0.016$, (c) $x = 0.0216$, (d) $x = 0.0244$, (e) $x = 0.032$, and (f) $x = 0.040$. Inset: a magnified view of κ near the spin-Peierls transition in zero field. The dashed line is an extrapolation of κ from above the transition temperature

In Figs. 1(e) and 1(f), a slight change in the curvature is observed at T_N and the field dependence in the Néel state is opposite to that above T_N ; κ decreases with field below T_N while κ increases with field above T_N . The three-dimensional magnon excitations, which appear in the Néel state, are responsible for this behavior. The thermal conductivity in U-AF phase will be further discussed elsewhere.¹⁵ Although the Néel transition (to D-AF phase) should be present also for the $x \leq x_c$ samples, we cannot identify the corresponding feature at the transition, because T_N ($\sim 2 - 2.5$ K)⁶ is too close to the lower temperature limit of our measurement, ~ 2 K.

Taking a look at the full scale of each figure, one can notice that κ is strongly suppressed with Mg substitution in the whole temperature range. Two thermal conductivity peaks are present in the zero-field curve of Fig. 1(a); one is in the SP phase and the other is in the 1D-QSL state. The broad shape of the high-temperature peak is maintained with doping. On the other hand, the low-temperature peak (SP peak) diminishes with $x \leq x_c$, and disappears for the $x > x_c$ samples.

The SP peak is suppressed also in magnetic fields [Figs. 1(a)-1(d)]. In order to see the field dependence in more detail, the thermal conductivity at the SP peak is plotted as a function of magnetic field in Fig. 2 for the $x = 0$ sample. κ is suppressed with magnetic field and suddenly drops at the threshold field, H_c , at which the system makes a transition to the incommensurate phase. The same features were observed in our previous measurement with the crystal grown by the laser-heated pedestal growth technique.¹¹ Also, the typical value of κ , for example at the high-temperature peak, is almost the same as that of the previous result. We thus believe that the above features are intrinsic in this material regardless of the growth method of the crystal, as long as high quality single crystal is used.¹⁴

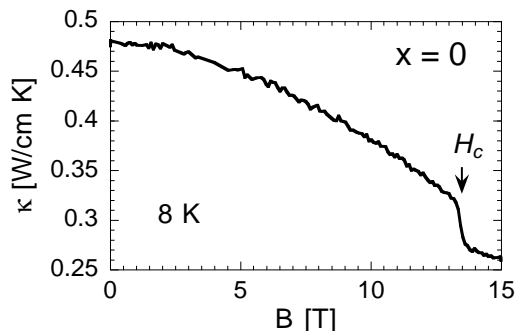


FIG. 2. Magnetic field dependence of the thermal conductivity at 8 K for pure CuGeO_3 , demonstrating the suppression of the low-temperature peak with field application.

In a temperature range close to T_{SP}^x , κ increases with field for the Mg-doped samples, while little field dependence is seen in the pure sample [Figs. 1(a)-1(d)]. Note that the field dependence extends even above T_{SP}^x for the Mg-doped samples. The variation in the field dependence implies qualitative difference of the SP transition between pure CuGeO_3 and doped CuGeO_3 . This field dependence is apparent also in the $x = 0.032$ sample, which is above x_c [Fig. 1(e)], but rapidly diminishes in the heavily doped sample [Fig. 1(f)].

IV. DISCUSSION

CuGeO_3 is an insulator and heat conduction by electrons or holes is absent unlike metals. Instead, low-energy spin excitations¹⁶ can carry heat. In the 1D-QSL state, total κ is given by a sum of κ_s and κ_{ph} as,

$$\kappa = \kappa_s + \kappa_{\text{ph}} \quad (\text{in 1D-QSL, } T_{\text{SP}} < T \ll J). \quad (1)$$

In contrast, κ_s is suppressed at the lowest temperature region in SP phase because few spin excitations are present due to the spin gap, and the total κ represents a phonon contribution only,

$$\kappa \sim \kappa_{\text{ph}} \quad (T \ll T_{\text{SP}}). \quad (2)$$

The field and impurity dependence of κ_{ph} below T_{SP} will be discussed in subsection A. The value of κ_s in 1D-QSL will be crudely estimated in subsection B. Finally, the problem of local spin-gap formation will be dealt with in subsection C, using this κ_s as a probe.

A. κ below T_{SP} : depression of the SP peak in magnetic fields and with Mg-doping

Since the low-temperature peak is drastically suppressed with the application of field as shown in Figs. 1 and 2, the feature should be related to the spin-excitation spectrum. We have proposed the following explanation for this peak.¹¹ At temperatures well below T_{SP} , where low-energy spin excitations are negligible, heat is carried mostly by phonons and κ_{ph} increases with temperature because of the growing population of phonons like usual insulating crystals. With increasing temperature, the increasing number of thermally excited spin excitations scatter phonons, and κ_{ph} diminishes. As a result, the thermal conductivity peak shows a peak. Although the thermal spin excitations begin to carry heat, the increase in κ_s appears only in the temperature region slightly below T_{SP} [see inset in Fig. 1(a)].

In order to confirm the above understanding, the impurity substitution is helpful because the spin gap is absent in heavily substituted samples. We normalized the size

of the peak for each sample as $\kappa(5\text{ K})/\kappa(15\text{ K})$, and plotted it against x in Fig. 3. One can see the suppression of the peak with x similarly to the case of field application (Fig. 2). Moreover, the peak disappears at the concentration $x > x_c$ where the long-range SP order no longer exists, as shown in Figs. 1(e) and 1(f). We have thus confirmed the correlation between spin gap and the peak also by Mg substitution, giving the additional evidence for the scenario described in the previous paragraph.

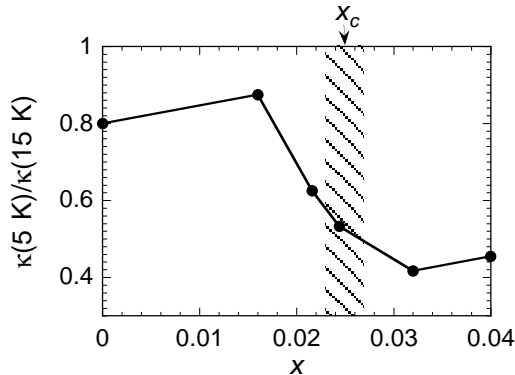


FIG. 3. A normalized size of the low-temperature peak, $\kappa(5\text{ K})/\kappa(15\text{ K})$, is plotted against Mg-concentration. A suppression of the peak with Mg doping is evident.

The $x = 0.0244$ sample, which is on the border from SP (D-AF) to U-AF demonstrates enhancement of κ below T_{SP}^x , as observed in Fig. 1(d). Since the enhancement is suppressed in magnetic fields, the existence of a well-defined spin gap is suggested even at $x = x_c$. We can notice the rapid change in κ_s in the (low-temperature) vicinity of T_{SP} , which is another sign of the spin-gap opening, for the $x = 0$ and 0.016 samples [Figs. 1(a) and 1(b)]. However, this feature is absent for the $x = 0.0216$ and 0.0244 samples [Figs. 1(c) and 1(d)], since κ_s is significantly reduced with x because of impurity scattering.

Figure 4(a) shows the zero-field thermal conductivity of all the samples. The thermal conductivity is strongly suppressed with Mg-substitution in the whole measured temperature range. The x dependence of κ below $\sim 4\text{ K}$ can be understood as the difference in the scattering rate of phonons. Since we showed in Ref. 11 that the scattering by planer defects is dominant for the $x = 0$ sample, difference in the number of planer defects may cause the variation of κ_{ph} in our series of samples. The number of planer defects does not necessarily increase with increasing x ; note that κ in the $x = 0.032$ sample is smaller than that in the $x = 0.040$ sample below $\sim 5\text{ K}$.

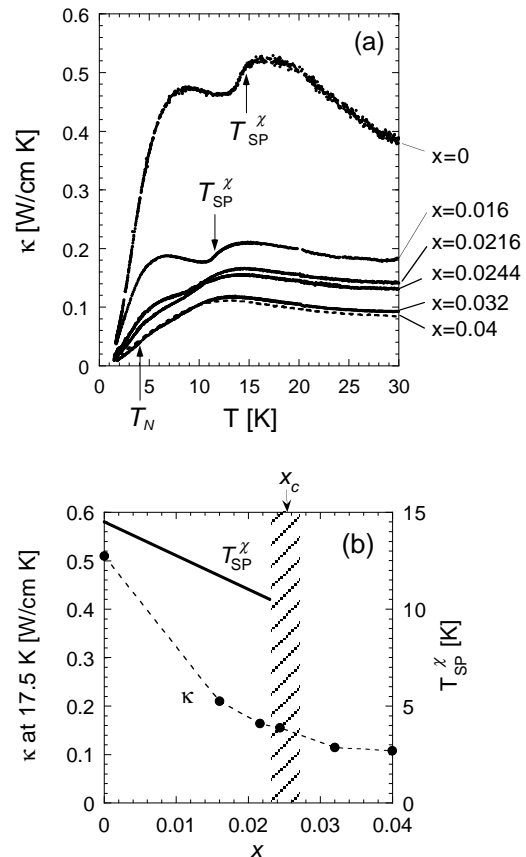


FIG. 4. (a) Temperature dependence of the zero-field thermal conductivity of $\text{Cu}_{1-x}\text{Mg}_x\text{GeO}_3$ single crystals. (b) The thermal conductivity at 17.5 K as a function of Mg concentration. The spin-Peierls temperatures measured by dc susceptibility are plotted together.

B. κ above T_{SP} : coherent heat transport in the 1D-QSL

Remembering the origin of the low- T thermal conductivity peak, we can notice that scattering by the spin excitations, in turn, becomes dominant in κ_{ph} above the peak temperature for the $x \leq x_c$ samples. Noting that all the $x \geq 0.016$ curves look parallel to one another above $\sim 15\text{ K}$, κ_{ph} in the $x > x_c$ samples should probably have a temperature dependence similar to that in the $x = 0.016$, 0.0216 and 0.0244 samples above $\sim 15\text{ K}$. Therefore, it is expected that phonon heat transport is governed by the spin-scattering also for the $x > x_c$ samples, at least above $\sim 15\text{ K}$.

In contrast to rather complicated temperature dependence below T_{SP} , $\kappa(T)$ in the 1D-QSL region is simpler, which is an advantage of discussing x dependence in the region. As a crude approximation, it is assumed that the phonon part is not so much x dependent and that most of the x -dependence comes from κ_s , because the detailed characterization¹² guarantees good homogeneity in both pure and Mg-doped crystals and the direct modification in the phonon modes due to the Mg substi-

tution can be estimated to be negligible. The scattering rate of phonons due to the point defects is more than two orders of magnitude smaller than the total scattering rate.¹⁷ One may notice that the robustness of κ_{ph} to the Mg-doping is natural, considering that phonons are mainly scattered by spin excitations above ~ 15 K, which is the conclusion of the previous paragraph. Since the population of both phonons and spin excitations does not change so much with x in the temperature range above T_{SP} , as has been reported in specific heat results,^{4,18,19} x dependence of κ_{ph} is expected to be small in the 1D-QSL state.²⁰

Figure 4(b) shows the x dependence of κ at 17.5 K. κ rapidly decreases with x up to x_c , and it saturates when x exceeds x_c . Therefore, it is naturally assumed that κ_s is close to zero in the heavily doped samples with $x > x_c$. This result suggests some correlation between the mobility of the spin excitations and the SP ordering.

Following the above interpretation, it is possible to estimate κ_s by subtracting κ of the $x = 0.040$ sample from the measured κ for each sample. The result indicates that most part of the κ of pure CuGeO_3 is due to κ_s , which is approximately 0.4 W/cm K at 17.5 K. This gives the diffusivity of the spin excitations D_s of $\sim 1.6 \times 10^{-3}$ m²/s, if we assume $C_s \sim 1.8$ J/mol K.¹¹ D_s in 1D systems can be written as $v_s l_s$, where v_s is the velocity of the spin excitations and l_s is the mean free path, in other words, the spin diffusion length. Assuming the spin-wave like dispersion given by des Cloizeaux and Pearson¹⁶ $\epsilon = (\pi/2)J_c |\sin(kc)|$ and $J_c \sim 120$ K,¹³ one can evaluate $v_s \sim (\pi/2)cJ_c/\hbar = 1.3 \times 10^4$ m/s and $l_s \sim 130$ nm (ϵ is the energy of the spin excitations, k is the wave vector and c (~ 0.3 nm) is the distance between adjacent spins). Note that the spin diffusion length of the same order of magnitude was obtained from the NMR relaxation measurement for another 1D spin system, AgVP_2S_6 .²¹

Since $l_s/c \sim 430$ is much larger than unity, we can conclude that the spin heat transport for the pure CuGeO_3 is coherent. If the same estimation is applied also to the Mg-doped samples, $l_s/c \sim 100$ for the $x = 0.016$ ($< x_c$) and $l_s/c \sim 50$ even for $x = x_c$ at this temperature. Since c/x_c is approximately calculated as 40, the above estimation indicates that the spin diffusion length in the 1D-QSL state exceeds the mean impurity distance c/x , as long as x is less than x_c . Whereas, the spin excitations are not so mobile when $x > x_c$.

C. κ just above T_{SP}^x : short-range SP order

Figure 5 shows $\kappa - \kappa(x = 0.040)$ ($\equiv \Delta\kappa$) of the three Mg-doped samples which have SP transition. One can find that $\Delta\kappa$ is almost temperature independent above $T^* \sim 15$ K and that $\Delta\kappa$ of all the samples deviates from this temperature-independent value below T^* . Since T^* is close to T_{SP} of the pure CuGeO_3 , the deviation can be attributed to a precursor of the SP transition. Note

that similar behavior is observed in the Raman scattering measurement on Zn- and Si-doped CuGeO_3 .²²

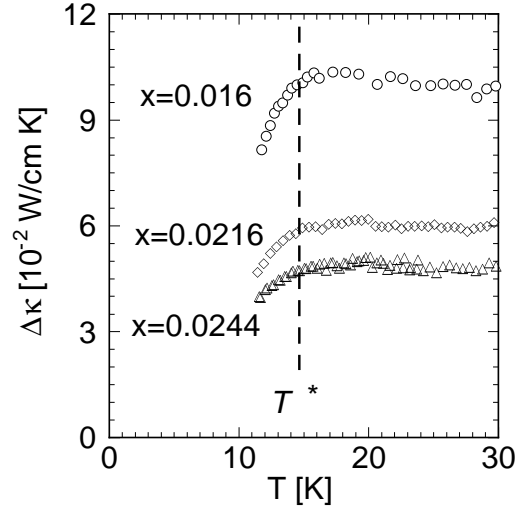


FIG. 5. Temperature dependence of $\Delta\kappa$ [$\equiv \kappa - \kappa(x = 0.040)$], for the $x = 0.016$, 0.0216 and 0.0244 samples. The local spin gap opens below ~ 15 K in all the samples.

Recently, it is shown by synchrotron x-ray diffraction measurement that FWHM of the Bragg peak from the lattice dimerization reaches the resolution limit at a temperature $T_{\text{SP}}^{\text{x-ray}}$ which is far below T_{SP}^x .²³ The authors claimed that the long-range order takes place only below $T_{\text{SP}}^{\text{x-ray}}$ and that lattice dimerization is short-range just below T_{SP}^x .²³ The gap-like feature in κ is also to be explained along the idea of the short-range order (SRO). However, the data in Fig. 5 suggests that SRO grows from $T^* \sim 15$ K, which is even above T_{SP}^x .

The field dependence of κ is a strong indication of the presence of the SRO below T^* . Figure 6 shows the temperature dependence of $\Delta\kappa$ for Mg-doped samples in various magnetic fields. In all cases, we observed the recovery of $\Delta\kappa$ with increasing fields below T^* . The results are consistent with the notion that the reduction of $\Delta\kappa$ below T^* is due to the development of the local spin gap. Since the magnetic field is thought to reduce the magnitude of spin gap even above T_{SP}^x , the number of spin excitations responsible for the heat transport will increase with the field. Moreover, the field dependence only appears below T^* in our observation. We have no field dependence above T^* , which is consistent with the notion that even the local spin gap is absent.

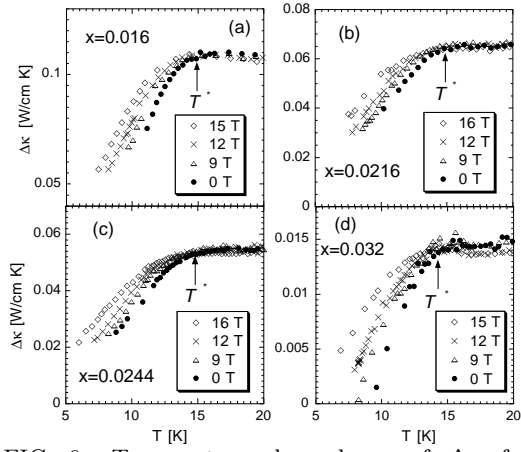


FIG. 6. Temperature dependence of $\Delta\kappa$ for the (a) $x = 0.016$, (b) $x = 0.0216$, (c) $x = 0.0244$ and (d) $x = 0.032$ samples. Magnetic fields are applied along the chain direction.

It should be emphasized that the heat transport by spin excitations is very sensitive to the spin-Peierls SRO. We observed a magnetic field dependence in $\Delta\kappa$ below T^* even for the sample with $x = 0.032$ ($> x_c$), where the spin-Peierls LRO no longer exist in the whole temperature range. According to the synchrotron x-ray measurement, SP-SRO develops below 7.5 K in the $x = 0.032$ sample.²³ For the $x = 0.040$ sample, however, there was no evidence that SP-SRO actually develops. In contrast, one can see that the magnetic field dependence of κ still exists for the $x = 0.040$ sample (Fig. 1(f)) even though the change is not so obvious as in the $x = 0.032$ sample. We think that the difference of a length scale of probed area between the two measurement techniques causes such discrepancy.

The above results tell us that the impurity-substitution modifies the ground state and suppresses the spin-Peierls ordering in CuGeO_3 system through different mechanisms. The importance of the inter-chain coupling and the tendency to the 3D-antiferromagnetism increases below $\sim T_N$. As a result, T_N increases with x and the ground state changes from D-AF to U-AF at x_c .²⁴ On the other hand, the local spin-gap formation, which occurs at T^* , is governed only by one-dimensional nature of the spin system coupled with 3D phonons and has nothing to do with 3D-AF fluctuation. Therefore, the temperature of SP-SRO is not modified with x , as long as the spin-singlet state is energetically favored. (the spin-singlet state will be no more favored in a heavily disordered system where long-wave-length spin excitations, whose energy is less than the spin-gap energy, are absent.²⁵) The spin-diffusion length l_s , in turn, rapidly diminishes with x owing to the growing impurity-scattering of the spin excitations. Since the spin correlation length is directly related to l_s ,²⁶ the length scale of the SP domains is reduced with x . As a result, signals of the spin gap, detected with any probe, diminishes in size with x .

V. SUMMARY

The thermal conductivity of the Mg-doped CuGeO_3 helps to understand both the spin-gapped state below the SP transition and the 1D-QSL state above the transition. Large spin heat transport is observed in the 1D-QSL state for pure CuGeO_3 , and rapidly diminishes with Mg-doping, accompanied by the suppression of the long-range SP ordering. The spin gap opening suppresses κ_s and enhances κ_{ph} . Examining the x dependence of the spin-gap features, it turned out that the local spin gap opens at a temperature (T^*) independent of x , suggesting that the suppression of SP ordering is attributed to the reduction of the spin diffusion due to the impurity scattering. It is expected that the above analysis of the impurity-substitution effect on the thermal conductivity is applicable to other one-dimensional spin systems and that thus obtained transport properties may reveal new aspects on such materials.

VI. ACKNOWLEDGMENT

We thank A. Kapitulnik for helpful advices both on the experimental techniques and in understanding the results in the early stage of this project.

APPENDIX: PHONON SCATTERING RATE DUE TO POINT DEFECTS

We can show that the scattering rate $1/\tau_p$ by point defects, which is introduced by the substitution with the ion with different mass, is very small even for the most heavily doped sample ($x = 0.040$). The dominant-phonon approximation gives,¹⁷

$$1/\tau_p \sim \frac{na^3(k_B T)^4}{4m\pi v^3 \hbar^4 (\Delta M/M)^2}. \quad (\text{A1})$$

[n ($= x = 0.040$) is density ratio of point defects, a ($\sim 4 \times 10^{-8}$ cm) is lattice constant, m ($= 15$) is number of phonon modes (3 times the number of atoms per unit cell), v ($\sim 5 \times 10^5$ cm/s) is phonon velocity and $\Delta M/M$ ($= 0.62$) is the ratio (mass difference between Mg and Cu atoms)/(mass of Cu atom)]. $1/\tau_p$ can be estimated to be about 1.0×10^8 (s^{-1}) at 30 K.

In comparison, the total scattering rate $1/\tau$ for the $x = 0.040$ sample can be obtained from the data as

$$1/\tau \sim \frac{C_{\text{ph}} v^2}{3\kappa_{\text{ph}}}, \quad (\text{A2})$$

assuming phonon specific heat C_{ph} to be $\sim \beta T^3$ and using the value of $\beta \sim 2.8 \times 10^{-6}$ ($\text{J}/\text{cm}^3 \text{K}^4$), shown in Ref. 11. Taking $\kappa_{\text{ph}} \sim 0.1$ ($\text{W}/\text{cm K}$) from our result of the κ measurement, $1/\tau \sim 6.4 \times 10^{10}$ (s^{-1}) at 30 K. Since

this $1/\tau$ is more than 600 times larger than $1/\tau_p$ (the ratio is even larger below 30 K), the scattering by the point defects is not important for the three-dimensional phonon heat transport in the measured temperature range.

-
- ¹ M. Hase, I. Terasaki, and K. Uchinokura, Phys. Rev. Lett. **70**, 3561 (1993).
- ² M. Hase, I. Terasaki, Y. Sasago, K. Uchinokura, and H. Obara, Phys. Rev. Lett. **71**, 4059 (1993).
- ³ M. Hase, N. Koide, K. Manabe, Y. Sasago, K. Uchinokura, and A. Sawa, Physica (Amsterdam) **215B**, 164 (1995).
- ⁴ S. B. Oseroff, S.-W. Cheong, B. Aktas, M. F. Hundley, Z. Fisk, and L. W. Rupp, Jr., Phys. Rev. Lett. **74**, 1450 (1995).
- ⁵ S. Inagaki and H. Fukuyama, J. Phys. Soc. Jpn. **52**, 3620 (1983).
- ⁶ T. Masuda, A. Fujioka, Y. Uchiyama, I. Tsukada, and K. Uchinokura, Phys. Rev. Lett. **80**, 4566 (1998).
- ⁷ Y. Sasago, N. Koide, K. Uchinokura, M. C. Martin, M. Hase, K. Hirota, and G. Shirane, Phys. Rev. B **54**, R6835 (1996).
- ⁸ M. C. Martin, M. Hase, K. Hirota, G. Shirane, Y. Sasago, N. Koide, and K. Uchinokura, Phys. Rev. B **56**, 3173 (1997).
- ⁹ H. Fukuyama, T. Tanimoto, and M. Saito, J. Phys. Soc. Jpn. **65**, 1182 (1996).
- ¹⁰ K. M. Kojima, Y. Fudamoto, M. Larkin, G. M. Luke, J. Merrin, B. Nachumi, Y. J. Uemura, M. Hase, Y. Sasago, K. Uchinokura, Y. Ajiro, A. Revcolevschi, and J. P. Renard, Phys. Rev. Lett. **79**, 503 (1997).
- ¹¹ Y. Ando, J. Takeya, D. L. Sisson, S. G. Döttinger, I. Tanaka, R. S. Feigelson, and A. Kapitulnik, Phys. Rev. B **58**, R2913 (1998).
- ¹² T. Masuda, I. Tsukada, K. Uchinokura, Y. J. Wang, and V. Kiryukhin, R. J. Birgeneau, Phys. Rev. B, **61**, 4103 (2000).
- ¹³ M. Nishi, O. Fujita, and J. Akimitsu, Phys. Rev. B **50**, R6508 (1994).
- ¹⁴ Recently, Vasil'ev *et al.* reported κ of CuGeO₃ single crystal, which does not show the low-temperature peak [A. M. Vasil'ev, M. I. Kaganov, V. V. Pryadun, G. Dhahenne, and A. Revcolevschi, JETP Lett. **66**, 868 (1997); A. M. Vasil'ev, V. V. Pryadun, D. I. Khomskii, G. Dhahenne, A. Revcolevschi, M. Isobe, and Y. Ueda, Phys. rev. Lett. **81**, 1949 (1998)]. Considering the fact that the absolute value of κ is smaller compared to our result, the absence of the peak is probably because of larger defect-scattering of phonons in their crystals.
- ¹⁵ J. Takeya *et al.*, in preparation.
- ¹⁶ J. des Cloizeaux and J. J. Pearson, Phys. Rev. **128**, 2131 (1962).
- ¹⁷ R. Berman, *Thermal Conduction in Solids* (Oxford University Press, Oxford, 1976), p. 73.
- ¹⁸ T. Lorenz, H. Kierspel, S. Kleefisch, B. Bücher, E. Gamper, A. Revcolevschi, and G. Dhahenne, Phys. Rev. B **56**, R501 (1997).
- ¹⁹ T. Masuda *et al.*, in preparation.
- ²⁰ It is hardly possible to assume that defect scattering is mainly responsible in κ_{ph} in the 1D-QSL state and that it causes the parallel shift in the $\kappa(T)$ curves for the $x \geq 0.016$ samples, because such scattering provides $\kappa_{\text{ph}}(T)$ proportional to T^2 .
- ²¹ M. Takigawa, T. Asano, Y. Ajiro, M. Mekata, and Y. J. Uemura, Phys. Rev. Lett. **76**, 2173 (1996).
- ²² H. Kuroe, H. Seto, J. Sasaki, T. Sekine, N. Koide, Y. Sasago, K. Uchinokura, M. Hase, M. Isobe, and Y. Ueda, J. Magn. Magn. Mater. **177-181**, 679 (1998).
- ²³ Y. J. Wang, V. Kiryukhin, R. J. Birgeneau, T. Masuda, I. Tsukada, and K. Uchinokura, Phys. Rev. Lett. **83**, 1676 (1999).
- ²⁴ M. Saito and H. Fukuyama, J. Phys. Soc. Jpn, **66**, 3259 (1997).
- ²⁵ G. S. Uhrig, F. Schönfeld, J-P. Boucher, and M. Horvatić, Phys. Rev. B **60**, 9468 (1999).
- ²⁶ B. I. Halperin and P. C. Hohenberg, Phys. Rev. **177**, 952 (1969).